

# Applied Mathematics NOTES

## de Mathématiques Appliquées

June 1983  
CONTENTS  
Articles

Vol. 8, No. 2

Juin 1983  
CONTENUE  
Articles

### Quaternionic Astroids and Starfields

John A. R. Holbrook . . . . .	1
Rough Edge of Math Leads to Scenery by Computer	
Derek York . . . . .	35

QUATERNIONIC ASTEROIDS AND STARFIELDS

John A. R. Holbrook  
Mathematics and Statistics  
University of Guelph

APPLIED MATHEMATICS NOTES  
NOTES DE MATHÉMATIQUES APPLIQUÉES

Editor

W.R. Smith  
Department of Mathematics and Statistics  
University of Guelph  
Guelph, Ontario N1G 2W1

Rédacteur

The Applied Mathematics Notes does not publish technical research papers designed for specialized audiences. We do solicit carefully written manuscripts on the following topics:

- Expository articles
- Unusual mathematical models
- Applications of mathematics
- New curricula in applied mathematics
- Education notes
- Listings of preprints or technical reports

Les travaux techniques destinés aux spécialistes ne sont pas publiés dans les Notes de Mathématiques Appliquées. Toutefois, vous pouvez collaborer à la revue en envoyant des travaux soigneusement rédigés tels que des

- articles généraux
- modèles mathématiques peu communs
- applications nouvelles
- nouveaux programmes d'études en mathématiques appliquées
- notes pédagogiques
- listes de rapports techniques et d'articles à paraître

Published by:

Canadian Mathematical Society  
Société Mathématique du Canada  
577 King Edward Avenue  
Ottawa, Ontario, K1N 6N5  
Canada

Publiée par:

ISSN 0700-9224

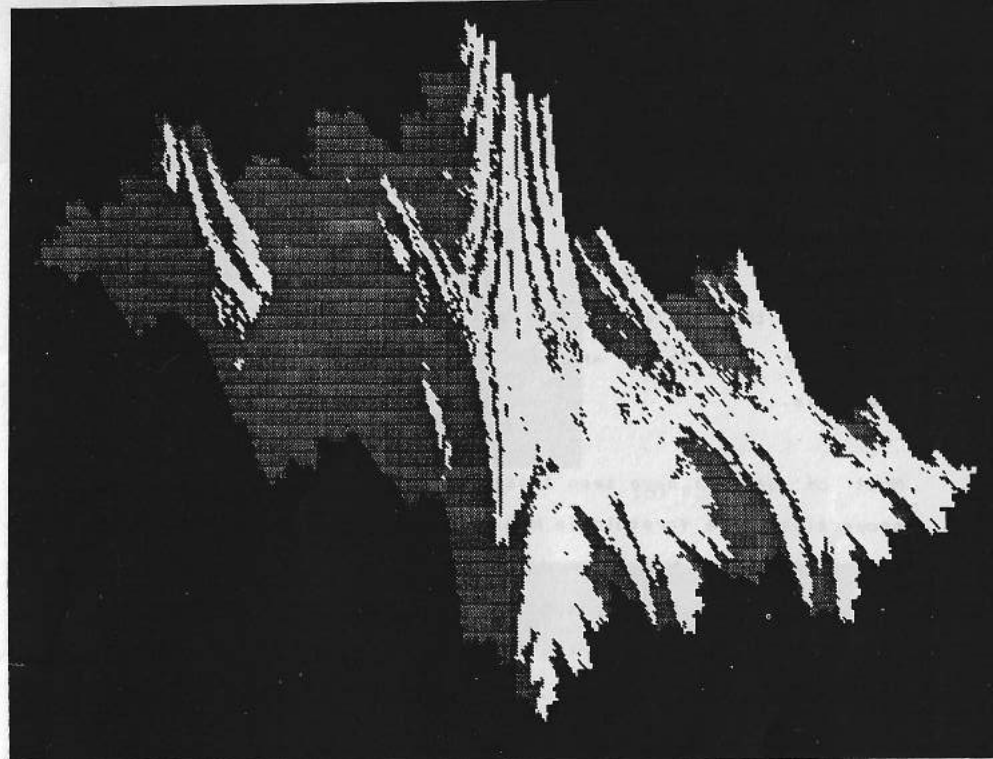


Figure 1: asteroid display of  $QFJ(.5, -.5, 0, 0)$

#### QUATERNIONIC ASTEROIDS AND STARFIELDS

John A. R. Holbrook  
Mathematics and Statistics  
University of Guelph

##### 1. Background

With the coming of modern computing techniques and equipment, we mathematicians are rich in new opportunities. Perhaps none is more important than our improved ability to communicate with nonmathematicians. Here computer graphics play the key role, allowing us to display something of the power and subtlety of mathematical ideas for all to appreciate. We should rejoice, then, that the fractal dragons brought to life by B. Mandelbrot\* have, for all their astonishing beauty, become a familiar spectacle.

Most of us will have seen these striking plane figures, whose properties were foretold in many respects by the classical work (c. 1920) of P. Fatou and G. Julia. Their studies of the iteration of rational mappings in the complex plane led Fatou and Julia to predict many of the remarkable features of the objects displayed in figure 2. Even so, one guesses that they themselves would have been surprised and delighted by the concrete embodiment of the objects. It is sad, then, to think that Fatou and Julia apparently were denied even the crude glimpses that are afforded by displays such as figure 2, now so easily obtained by any microcomputer with "high-resolution" graphics. How much more \*for a general introduction to Mandelbrot's work, see the next article

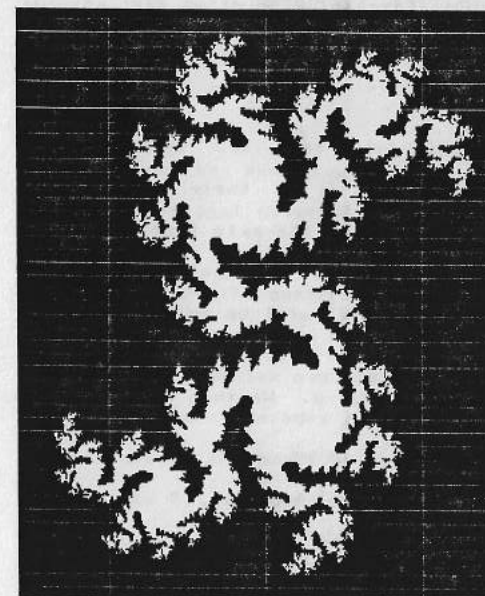
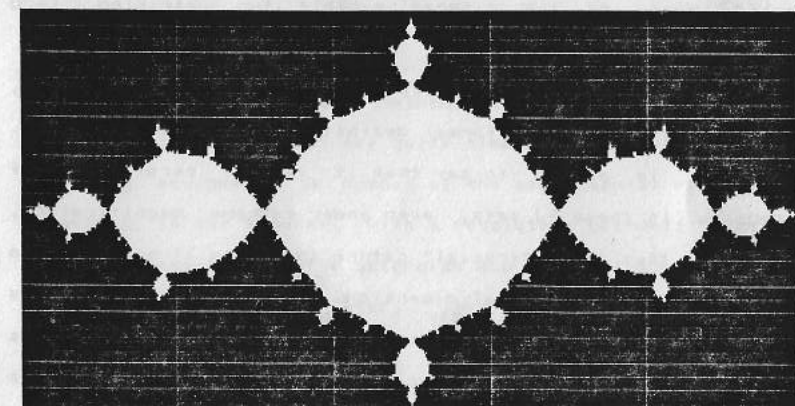


Figure 2

(a) FJ(-.378,.3072)



(b) FJ(1,0)

they would have enjoyed the superbly detailed, multicolored presentations available, for example, in Mandelbrot's "The Fractal Geometry of Nature" [5].

\*  
One of the charms of the Fatou-Julia sets (FJ sets) is the contrast between the utter simplicity of their mathematical description and the visual complexity of the sets themselves. The classical FJ sets are the stable sets of rational maps  $f(z)$  of the complex plane  $\mathbb{C}$  into itself, and it will be quite enough for our purposes to restrict to the case of a quadratic polynomial, which we may write in the form  $f(z)=z^2-\mu$ . We then describe the corresponding FJ set by

$$FJ(\mu) = \{z \in \mathbb{C} : f_n(z) \text{ remains bounded as } n \rightarrow \infty\},$$

where  $f_n$  denotes the  $n$ -fold composition of the map  $f$  with itself. Merely by varying the single complex parameter  $\mu$ , one obtains an astonishing variety of figures  $FJ(\mu)$ , each one remarkable in itself. Most of the figures exhibit two striking (and interacting) features: fractal dimension and self-similarity. Since this article will stress exploration rather than analysis, we will not try to give formal definitions of these features. Perhaps it is enough to say that it is the persistence of jaggedness in these FJ sets, even under extreme magnification, that gives them their "fractal" nature and makes it necessary to assign to them a nonintegral dimension. "Self-similarity" refers to a phenomenon evident in many of the illustrations in this article: down to the smallest scale there are parts of the

objects that (with only inessential distortion) repeat the shape of the object as a whole. For a more satisfying discussion of these concepts we refer the reader to Mandelbrot's book [5].

The impulse to expand these constructions from the plane to higher-dimensional spaces is almost irresistible, and there is a "natural" way to try doing it: use quaternions in place of complex numbers. The quaternions make  $\mathbb{R}^4$  into a normed skew field (sometimes denoted by  $\mathbb{H}$ , in honor of W. R. Hamilton) that contains the complex numbers as a substructure. They were hot stuff for several decades in the last century; see the entries on quaternions in the books by E. T. Bell [1] and F. Klein [4], the treatise by P. G. Tait [7], and the more specialized articles by C. A. Deavours [2] and by S. Eilenberg and I. Niven [3]. Quaternions often rate only a passing reference in the current mathematical curriculum. The phenomena associated with "quaternionic FJ sets" should renew curiosity about the structure of  $\mathbb{H}$ .

This article describes some methods of computing and displaying quaternionic FJ sets that are quite simple to implement on modest computing equipment. A number of the experimental results are presented in the figures, with a resolutely gee-whiz attitude. Good explanations of the asteroids and starfields we see here will perhaps be supplied later.

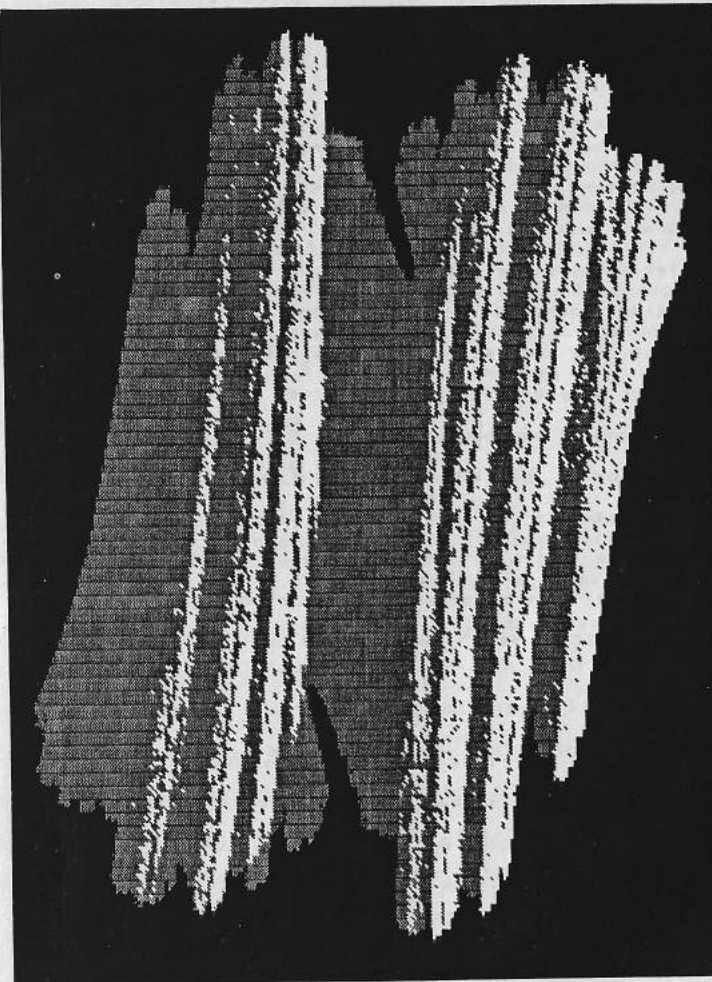


Figure 3: asteroid display of QFJ(-.378,.3072,0,0)

Without doubt, variations of these methods have been studied by other mathematicians, although the only specific reference we have at the moment is to work by Alan Norton\*, described in a popular account of fractals by K. Stein [6]. Most of the programs used in this investigation were originally written in BASIC and run on a standard microcomputer and dot-matrix printer. Later, to quicken the exploration and make it easier to get displays suitable for reproduction, the computational programs were reworked in FORTRAN and run on a big machine. Many thanks to Jean-Pierre Schoch for his help at that stage.

## 2. Quaternionic Fatou-Julia Sets

Recall that a quaternion  $q$  is a real 4-vector  $(x,y,z,t)$  with the understanding that quaternions are added like 4-vectors but multiplied as follows: for  $q,q' \in \mathbb{H}$ ,

$$qq' = (xx' - yy' - zz' - tt', xy' + yx' + zt' - tz', xz' + zx' + ty' - yt', xt' + tx' + yz' - zy').$$

It turns out that this structure is a skew field and that the special quaternions of the form  $(x,y,0,0)$  behave like complex numbers  $x+iy$ . Of the many interesting properties of  $\mathbb{H}$ , we need to recall only a few. The usual Euclidean distance in  $\mathbb{R}^4$  yields a multiplicative norm  $|q|$  on  $\mathbb{H}$ . Most quaternions have two square roots, easily computed (more about this later); exceptions are the real quaternions  $\pm 0$  (ie  $(x,0,0,0)$  with  $x \neq 0$ ), but for these we

\*but see the appendix to this article

may agree to choose the usual complex square roots (as imbedded in  $\mathbb{H}$ ).

Given a quaternion  $\mu$  (the basic parameter in our explorations), we may define the quadratic map  $f:\mathbb{H} \rightarrow \mathbb{H}$  by  $f(q)=q^2-\mu$ , and denote by  $f_n$  the  $n$ -fold composition of  $f$  with itself. Let

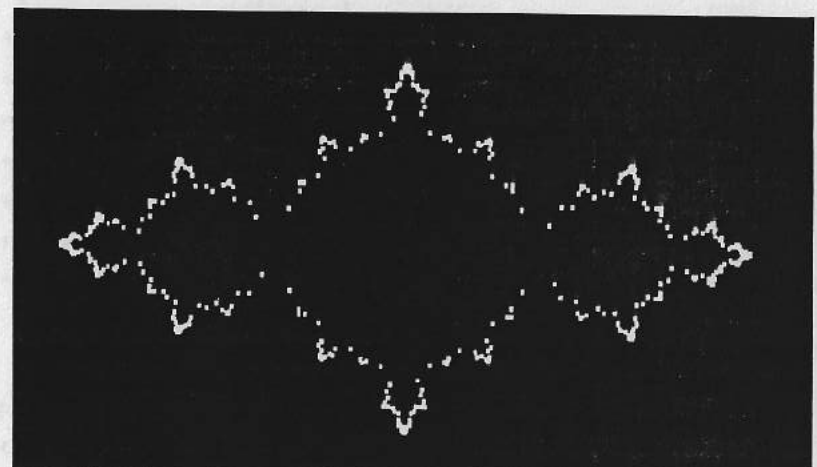
$$QFJ(\mu) = \{q \in \mathbb{H} : |f_n(q)| \text{ remains bounded as } n \rightarrow \infty\}.$$

In general, this will be a certain subset of  $\mathbb{H}$ , ie of 4-space. If our parameter  $\mu$  is complex, of the form  $(a,b,0,0)$ , it is clear that the  $x-y$  section of  $QFJ(\mu)$  will be the classical Fatou-Julia set  $FJ(a,b)$ , but even there the  $QFJ$  set as a whole will be fattened into the other two dimensions ( $z$  and  $t$ ). Thus figure 3 attempts to show how the famous dragon  $FJ(-.378,.3072)$  of figure 2 becomes fattened into the  $z$  dimension when regarded as a "quaternionic dragon".

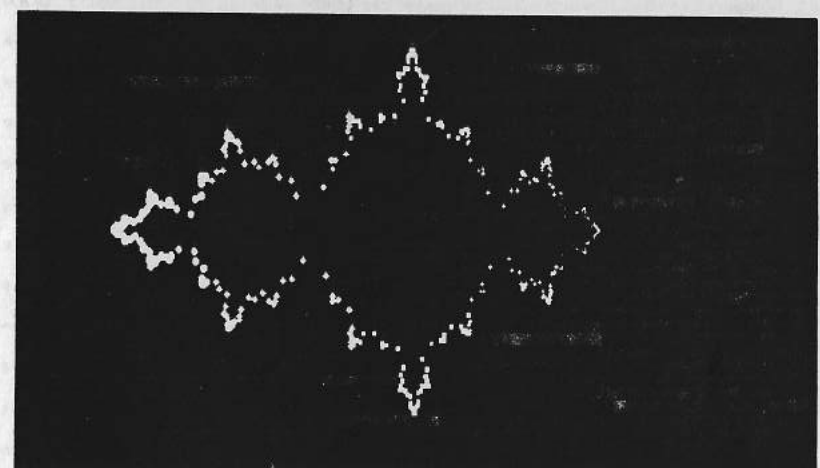
### 3. Two Methods of Display (Asteroids and Starfields)

Simple calculations with the norm on  $\mathbb{H}$  determine an "escape radius"  $r$  (depending on the parameter  $\mu$ ) such that whenever  $|q| > r$  the iterates of  $f$  carry  $q$  inevitably to infinity. Thus, for a given  $q$ , if there is some  $n$  such that  $|f_n(q)| > r$  then  $q$  is not in  $QFJ(\mu)$ . For an appropriately large  $N$ , we may expect that

$$A(\mu, N) = \{q \in \mathbb{H} \in \mathbb{R}^4 : |f_n(q)| \leq r \text{ for all } n \leq N\}$$



(a)



(b)

Figure 4: two starfield presentations of the (planar) QFJ set  $QFJ(1,0,0,0)$

will be a good approximation to  $QFJ(\mu)$ . The brute-force method of approximating  $QFJ(\mu)$  is therefore to choose an appropriately fine grid of points covering  $\{q: |q| \leq r\}$  and an appropriately large  $N$  and carry out the computations to determine which points in the grid lie in  $A(\mu, N)$ . This is the method that gives the objects of figure 2 (white regions display grid points in  $A(\mu, N)$  as a subset of the plane) and that is the basis of the "asteroid" presentations of approximate  $QFJ$  sets.

In the quaternionic case  $A(\mu, N)$  is a subset of 4-space and further steps are needed to produce a useful (two-dimensional) picture. We first take a time-slice (ie we look at a single instant in the life of our  $QFJ$  set): fix  $T$  and consider only grid points  $(x, y, z, t)$  with  $t=T$ . The corresponding  $(x, y, z)$  form a three-dimensional figure whose structure is partially revealed by simulating the light and shadow that would be seen if the figure were modelled in plaster and illuminated from the side. The resulting "asteroids", several of which are shown in the figures, should be interpreted as follows. We are looking at the slice as a solid object in xyz-space positioned in such a way that the origin is central and our line-of-sight is in the positive z-direction; the x- and y-axes lie in the page with the x-axis pointing right and the y-axis pointing "up"; we see the object against a black background of "deep space", with illumination coming from some revealing angle perpendicular to the y-axis (in most of the figures the light shines from a "sun" at infinite

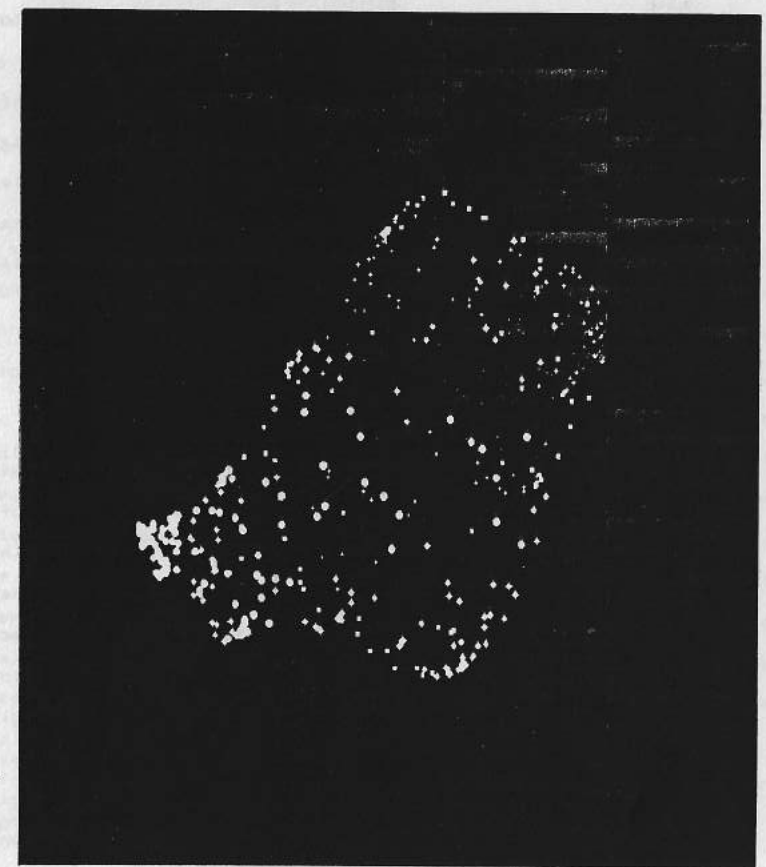


Figure 5: starfield display of  $QFJ(.4,.6,.35,0)$

distance in the direction of  $(2,0,-1)$ ; visible portions of the object that are in full sun are shown in white while those that are shaded by other parts of the object are shown in half-tone.

Quite a different approach is used to obtain the "starfield" displays of QFJ sets. This method involves much less computation, but its presentation of some QFJ sets may be rather misleading (see the next section). In this method an arbitrary starting point  $q_0$  is chosen (we have used  $q_0 = (1,1,0,0)$ ) and the inverse images

$$\begin{aligned} f^{-1}(q_0), f^{-2}(q_0) (=f^{-1}(f^{-1}(q_0))), \dots \\ \dots, f^{-N}(q_0) (=S(\mu, N)) \end{aligned}$$

are computed. Since  $f^{-1}(q)$  is simply the set of square roots of  $q+\mu$ , the number of points doubles at each stage of the computation, so that the last set  $S(\mu, N)$  consists of  $2^N$  points in 4-space. From these the "starfield" picture is obtained as follows. The points are projected onto the  $xyz$ -subspace by ignoring their  $t$ -coordinates. The resulting scatter of points in 3-space is then plotted within a cube centered at the origin and with the axes oriented as for the asteroid displays. The distribution of points is shown in perspective by shrinking distances in the more remote depths of the cube (in this process the back face of the cube is shrunk so that it appears to be one-half the size of the front face). The points are then displayed as white areas ("stars") against a black background, and to enhance the illusion of depth the more distant stars are reduced

in "magnitude", ie the size of the white area is made smaller. It was found to be convenient to allow rotation of the scatter of points (by an arbitrary angle about the  $y$ -axis) before computing the display as described above. In many cases this affords a better view of the starfield, and allows views of the same starfield from various angles.

To see how the method works out in a simple situation, consider figure 4. Here  $\mu = (1,0,0,0)$ , a "complex" quaternion. Since our starting point  $q_0$  for the inverse iterations is also in the complex  $xy$ -subspace, and since, as mentioned in the last section, we are careful to take only the complex roots of complex quaternions, it is clear that, in a case like this, the whole set  $S(\mu, N)$  will lie in the  $xy$ -subspace. Figure 4(a) shows the resulting planar starfield; it should, of course, correspond to the classical FJ(1,0), and reference to figure 2(b) shows that there IS a clear relationship. It is equally clear that figures 4(a) and 2(b) are systematically different; we discuss this difference in section 4. In figure 4(b) the starfield of figure 4(a) has been rotated 45 degrees out of the page ( $xy$ -plane) before display, and the effects of perspective and stellar magnitude are easy to note and interpret.

Figure 5 shows a "genuinely 3-dimensional" quaternionic starfield, corresponding to  $S((.4,.6,.35,0),9)$ .

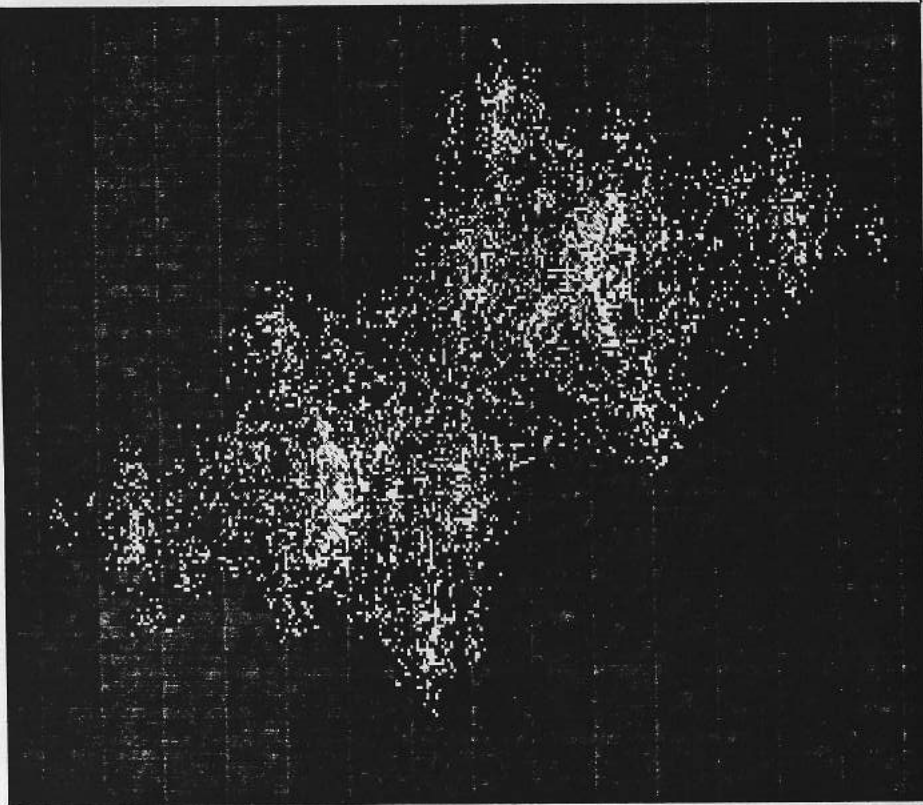


Figure 6: asteroid display of QFJ(.4,.6,.35,0)

#### 4. Problems of Interpretation

The figures generated by our methods should be viewed with some scepticism. In the first place, they are finite, discrete approximations to objects that depend on continuous and infinite processes. The value of  $N$  in our starfield displays of  $S(\mu, N)$  is typically 9, meaning that 512 stars might be made out in a well-scattered display. Because this  $N$  is not larger and because the display is based on a dot-matrix roughly 300x300, the starfield presentations are bound to be somewhat inaccurate as models of our QFJ sets. Likewise, our asteroid displays are typically based on a test-grid of 320x320 points and the number of iterations  $N$  that determine the sets  $A(\mu, N)$  must also be kept within reasonable bounds (we have often used  $N=50$ ). For these reasons, the asteroid displays too must be interpreted cautiously. But there are other, more subtle difficulties.

A comparison of figures 2 and 4 will suggest that the starfield (inverse iteration) method of approximating an FJ or QFJ set ignores the interior of the set. Indeed, it is known in the classical case (FJ sets) that the inverse images  $f^{-n}(z_0)$  will cluster on the outward projections of the set, just as an electric charge would be concentrated near the spikes and corners of an object. It is also known that, in the limit, the inverse images are dense in the boundary of the FJ set. Nevertheless, the concentration will be so much stronger on the salient features of

the object that, as a practical matter, it is hopeless to expect the starfield method to do justice to, for example, the marvelous fiords of figure 2(a). Similar effects seem to occur in the starfield displays of QFJ sets.

Other ambiguities in our displays stem from the varying fractal dimension of the  $QFJ(\mu)$ . For some choices of  $\mu$  the corresponding asteroids seem to be quite solid and substantial, even though they may be exceedingly intricate at the boundary; figure 1 shows a good example. In a mysterious way, other choices of  $\mu$  result in asteroids that are tenuous or ragged (see, for example, figures 6 and 7). Roughly speaking, as the norm of the parameter  $\mu$  increases, the corresponding  $QFJ(\mu)$  tends to be more diffuse or granular; compare figures 1 and 9.

No  $QFJ(\mu)$  can be empty; in fact, there must be many periodic points for the mapping  $f$ . To see this, note that any solution to the equation  $f_n(q) = q = 0$  will be periodic for  $f$  of period  $n$  (or some divisor of  $n$ ). The left-hand side of the equation is a polynomial  $p(q)$  in the quaternionic variable  $q$ , and there is an interesting version of the "fundamental theorem of algebra" for quaternions (see Eilenberg and Niven [3] for a proof). Since we are working in a noncommutative system, there may be many terms in  $p(q)$  of a given degree in  $q$  that cannot be combined in a single term; it is clear, however, that there is just a single leading term  $q^m$ , where  $m=2^n$ . The Eilenberg and Niven fundamental theorem ensures that each polynomial with a single term of

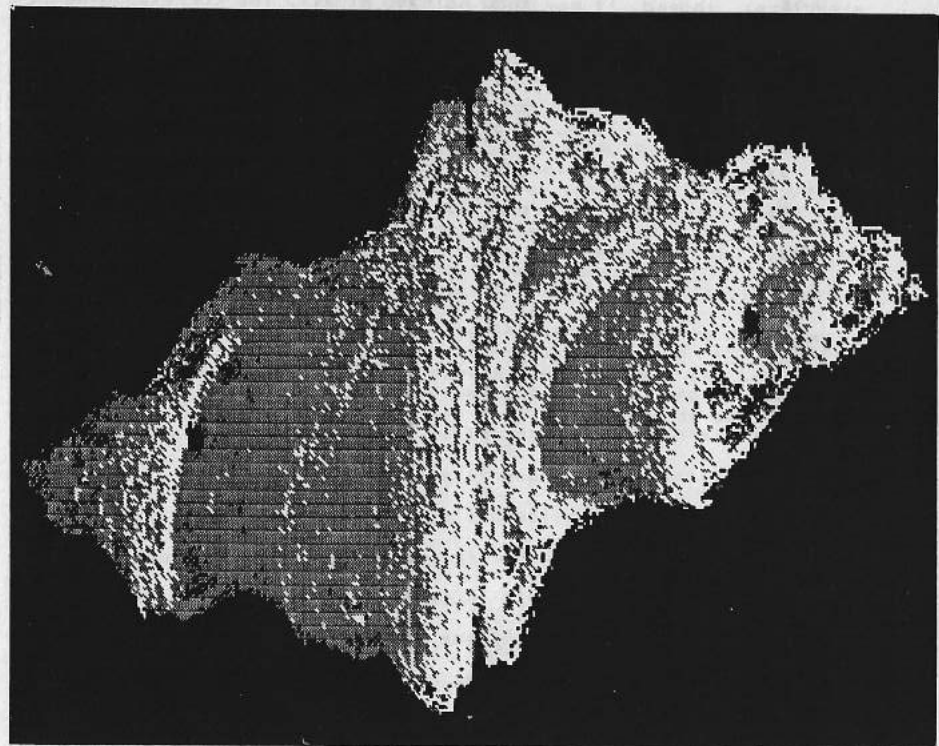


Figure 7: asteroid display of  $QFJ(.43,.43,.43,0)$

highest degree has a quaternionic root, so there are "lots" of periodic points.

Nevertheless, if the fractal dimension of QFJ( $\mu$ ) is small the asteroid method of display may give a very poor indication of its structure; indeed, it may show nothing at all. The corresponding starfield, on the other hand, gives no obvious signal when the QFJ is sparse; the starfield always displays roughly the same number of points. Thus, figures 5 and 6 represent the same QFJ set, except for a rotation of 35 degrees about the y-axis, but the starfield doesn't reveal the advanced dissipation of the asteroid. In a case such as this we must also wonder whether further iterations in the asteroid method might result in total evaporation of the display. Figure 10 shows the starfield display of a QFJ set that we would expect to register not at all when displayed as an asteroid.

##### 5. The Programs

Because it may be helpful to those readers who wish to conduct their own experiments along these lines, we provide listings of some programs of the type we have used. The versions listed are written in MBASIC and should run (albeit slowly!) on many microcomputers. Of course, the escape sequences used to pass the bit-image graphics to the printer are more specialized and readers will have to adapt those sections of the programs to

their own equipment.

We have tried to clarify the logic of the programs by inserting appropriate remarks in the listings themselves. Some comments, however, seem easier to make beforehand.

Program I is elementary and merely computes by the brute-force method the outline of the familiar Fatou-Julia sets, displaying them in a manner analogous to the asteroid method. Since everything is two-dimensional, there is no loss in information and the sets appear as white areas against a black background. With a compiled version (3 or 4 times faster), one gets pictures like those of figure 2 within a few hours.

Program II is logically the most intricate and requires the most computation. Even a compiled version will need many hours on a typical micro, but should yield asteroid presentations similar to the figures of this article (though less detailed, unless you have lots of machine memory and patience). No doubt the program could be accelerated somewhat by some simple rearrangement, but it is inherent in the logic of the program that the subroutine that estimates distance to the QFJ set must be called very often. The method used to obtain the illuminated asteroid display is quite primitive. For given values of x and y (determining the position on the display page) a "visual probe" is sent into the xyz cube containing the chosen time-slice of the QFJ set; ie test points  $(x,y,z)$  are introduced, with increasing values of z

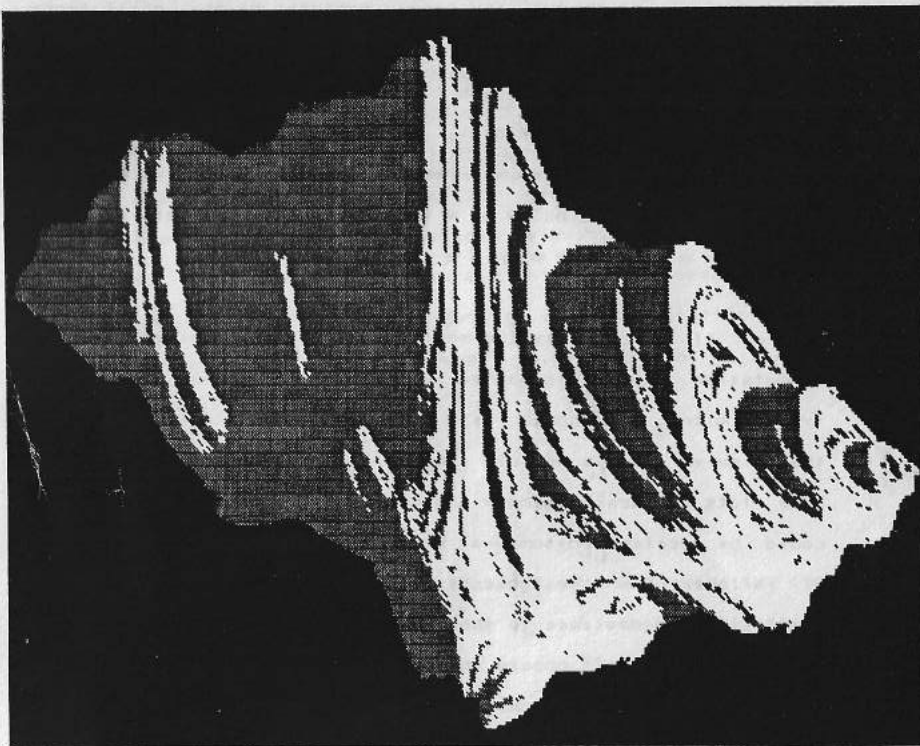


Figure 8: asteroid display of QFJ(.4,-.4,.4,0)

representing motion of the probe along the line-of-sight parallel to the z-axis. At each position the distance of  $\langle x,y,z,t \rangle$  to the QFJ set is estimated to determine how far we can advance without "jumping over" the set. If the set is never encountered, "deep space" is shown at the corresponding xy-position of the display. If the QFJ set IS encountered, the probe is sent back toward the "sun" (potential illumination); if the set is encountered a second time, shadow (half-tone) is shown at the original xy-position of the display.

Program III yields starfield displays of QFJ sets by the straightforward application of the inverse-image technique described earlier. Inversion of  $f$  entails the extraction of quaternionic square roots, which may be achieved as follows. Every quaternion  $q=\langle x,y,z,t \rangle$  can be written in the form  $x+nrm.U$ , where  $U$  is a vector  $\langle 0,U_1,U_2,U_3 \rangle$  of unit length and  $nrm$  is the length of  $\langle 0,y,z,t \rangle$ . This notation is meant to conform to that of program III (see lines 110-200 of the listing). The vector  $U$  is uniquely determined except when  $nrm=0$ ; by choosing  $U=\langle 0,1,0,0 \rangle$  in this exceptional case, we ensure that complex roots are obtained in the following process whenever we start with a complex  $q$ . In the quaternionic operations the vector  $U$  behaves like the imaginary unit  $i$ , ie  $U.U$  is (the real quaternion) -1. From this one sees that the quaternionic roots of  $q=x+nrm.U$  are just those  $a+b.U$  such that  $a+b.U$  is a root of  $x+nrm.i$  (in the usual complex sense). There are good and bad ways to compute the complex root  $a+b.U$ ; we have used  $a=(.5*(md+x))^{1/2}, b=(.5*(md-x))^{1/2}$ ,

where  $md=(x^2+nrm^2)^{1/2}$ , because this process is stable at the origin.

Program I

```
10 REM *** FJMU.BAS - DISPLAYS FJ SETS
20 INPUT "ENTER PARAMETER MU (M1,M2): ",M1,M2
30 INPUT "ENTER NUMBER OF ITERATIONS: ",N
40 INPUT "ENTER WIDTH OF DISPLAY (# OF DOTS < 601): ",W
50 DIM BYT(600)
60 REM *** R COMPUTES THE ESCAPE RADIUS
70 R=.52+SQR(.25+SQR(M1*M1+M2*M2))
80 REM *** DEL IS INTERNAL VALUE OF DOT SPACING
90 DEL=2*R/W
93 REM *** FOLLOWING LINES PREPARE PRINTER
95 LPRINT CHR$(27);CHR$(62);
97 LPRINT CHR$(27);CHR$(84);CHR$(49);CHR$(54);
100 REM *** I INDEXES ROW (8 DOTS HIGH) OF DISPLAY
110 FOR I=0 TO INT(W/8)
120 REM *** J INDEXES COLUMN OF DISPLAY
130 FOR J=1 TO W
140 REM *** BY WILL CODE THE I-J-TH 8-DOT SUBCOLUMN OF DISPLAY
150 BY=0
160 REM *** K INDEXES POSITION WITHIN SUBCOLUMN
170 FOR K=0 TO 7
180 REM *** X,Y GIVE COMPLEX Z CORRESPONDING TO DOT POSITION
190 X=-R+DEL*I;Y=R-DEL*(I*8+K)
```

[continued]

[program I, continued]

```
200 REM *** LINES IN 200-BLOCK APPLY F ITERATIVELY TO Z UP TO
202 REM *** N TIMES, MARKING BY WITH THE CORRESPONDING BIT IF
204 REM *** ESCAPE RADIUS R IS EXCEEDED
210 FOR L=0 TO N-1
220 IF R*R<(X*X+Y*Y) GOTO 250
230 XL=X*X-Y*Y-M1
235 Y=Z*X*Y-M2
240 X=XL
249 GOTO 290
250 BIT=2^K:BY=BY+BIT
260 L=N-1
290 NEXT L
300 NEXT K
305 REM *** NEXT PLACE DISPLAY DATA FOR J-TH SUBCOLUMN IN BYTE
310 BYTE(J)=BY
320 NEXT J
330 REM *** LINES 340-400 PRINT I-TH LINE OF DISPLAY (8 DOTS
332 REM *** HIGH) FROM DATA IN BYTE
340 FOR P=1 TO 3
343 FOR Q=1 TO 6
345 LPRINT CHR$(27);CHR$(83);CHR$(48);CHR$(54);CHR$(48);CHR$(48);
347 FOR J=1 TO 100*(Q-1):LPRINT CHR$(0);:NEXT
355 FOR J=100*Q-99 TO 100*Q
360 LPRINT CHR$(BYTE(J));
365 NEXT J
367 FOR J=100*Q+1 TO 600:LPRINT CHR$(0);:NEXT
369 LPRINT CHR$(13);
370 NEXT Q
380 NEXT P
400 LPRINT CHR$(13)
410 NEXT I
450 REM *** FOLLOWING LINE LABEL THE DISPLAY
460 LPRINT:LPRINT "FATOU-JULIA SET WITH MU = ";M1;M2
470 LPRINT:LPRINT "APPROXIMATION USING ";N;" ITERATIONS"
480 LPRINT:LPRINT "DISPLAY WIDTH IS ";W;" DOTS"
500 END
```



Figure 9: asteroid display of QFJ(.6,-.6,0,0)

Program II

```
10 REM **** QFJ.BAS - DISPLAYS QFJ ASTEROIDS
20 INPUT "ENTER MU (4-VECTOR): ",M1,M2,M3,M4
21 REM **** LM IS THE NORM OF MU; LINF IS THE ESCAPE RADIUS
22 LM=SQR(M1*M1+M2*M2+M3*M3+M4*M4)
24 LINF=.52+SQR(LM+.25)
25 REM **** T DETERMINES THE TIME-SLICE TO BE COMPUTED AND DISPLAYED
26 INPUT "ENTER 'TIME' (FIXED 4TH COORD OF Q): ",T
27 REM **** SA IS THE INTERNAL VALUE OF THE DISPLAY SEMI-AXIS
28 REM **** N=NUMBER OF DOTS ON EACH SIDE OF DISPLAY
29 REM **** DEL IS THE INTERNAL VALUE OF DOT SPACING
30 SA=LINF
40 INPUT "ENTER NUMBER OF INCHES ON SIDE OF PLOTTED CUBE (1,2,3,4,5, OR 6): ",IN
50 N=80*IN
60 DEL=SA/(40*IN)
70 REM *** VECTORS DS (DEEP SPACE) AND SH (SHADOW) WILL STORE THE
80 REM *** BYTES CONTAINING THE BIT-IMAGE GRAPHICS DATA REQUIRED TO
90 REM *** PRINT EACH LINE (8 DOTS HIGH) OF THE DISPLAY
100 DIM DS(500),SH(500)
109 REM **** NEXT LINE SETS PRINTER LINE-HEIGHT (ZERO SPACING)
110 LPRINT CHR$(27);CHR$(84);CHR$(49);CHR$(53);
120 INPUT "ENTER SLOPE OF INCIDENT LIGHT (INTEGER): ",S
122 HYP=SQR(1+S*S)
130 INPUT "ENTER NUMBER OF ITERATIONS OF F(Q)=Q*Q-MU: ",M
140 REM **** H INDEXES THE ROW (8 DOTS HIGH) OF DISPLAY
150 FOR H=1 TO 10*IN
155 REM **** J INDEXES THE COLUMN OF DISPLAY
156 REM **** 160-180 RESET DS AND SH TO ZERO
160 FOR J=1 TO N
170 DS(J)=0:SH(J)=0
180 NEXT J
200 FOR J=1 TO N
204 REM **** I INDEXES THE DOT POSITION IN THE 8-DOT J-TH COLUMN
205 REM **** (IN THE H-TH PRINT LINE); BI IS THE BIT CORRESPONDING
206 REM **** TO THIS POSITION (BI IS RESET IN 208)
208 BI=1
210 FOR I=1 TO 8
215 REM **** 220 COMPUTES THE INITIAL POSITION OF THE LINE-OF-SIGHT
216 REM **** THAT DETERMINES THIS DOT OF DISPLAY
220 Z=-SA:X=(J-40*IN)*DEL:Y=(40*IN-(8*(H-1)+I))*DEL
```

[continued]

[program II continued]

```

221 REM **** THE 230-270 LOOP ADVANCES THE POINT ON THE PROBING
222 REM **** LINE-OF-SIGHT BY THE 'DISTANCE' D (A LOWER BOUND ON THE
223 REM **** ACTUAL DISTANCE FROM THE CURRENT XYZ (AND T, FIXED) TO
224 REM **** THE QFJ SET; D IS COMPUTED BY THE SUBROUTINE AT 1000)
225 REM **** EXIT FROM THE LOOP IS EITHER TO 500, WHEN THE LINE-OF-
226 REM **** -SIGHT ENCOUNTERS THE QFJ SET, OR TO 700, WHEN IT BECOMES
227 REM **** CLEAR THAT THE SET IS NOT SEEN ALONG THAT LINE
230 GOSUB 1000
240 IF D<DEL/2 GOTO 500
250 Z=Z+D
260 IF Z>SA GOTO 700
270 GOTO 230
450 REM **** THE 500-560 LOOP COMES INTO PLAY AFTER THE QFJ SET HAS
451 REM **** BEEN SEEN ALONG A GIVEN LINE-OF-SIGHT; IT LOOKS BACK FROM
452 REM **** THE POINT OF INITIAL CONTACT, ALONG THE DIRECTION OF THE
453 REM **** (POTENTIAL) ILLUMINATION; EXIT FROM THE LOOP IS EITHER TO
454 REM **** 650, WHEN THE QFJ SET IS ENCOUNTERED AGAIN (650 ADJUSTS
455 REM **** SH(J) SO THAT THE CURRENT DOT OF THE DISPLAY WILL SHOW
456 REM **** SHADOW AT THE CORRESPONDING POINT ON THE ASTEROID), OR TO
457 REM **** 710 (GOES ON TO NEXT DOT POSITION, LEAVING THE CURRENT DOT
458 REM **** 'ILLUMINATED'); EXCEPT FOR THE FIRST STEP, THE PROBE IS
459 REM **** MOVED BY D (COMPUTED BY THE SUBROUTINE) TOWARDS THE 'SUN'
500 Z=Z-DEL:X=X+S*DEL
510 GOSUB 1000
520 IF D<DEL/2 GOTO 650
530 A=D/HYP
540 Z=Z-A:IF Z<-SA GOTO 710
550 X=X+S*A:IF X>SA GOTO 710
560 GOTO 510
650 SH(J)=SH(J)+BI:GOTO 710
690 REM **** 700 COMES INTO PLAY WHEN THE CURRENT LINE-OF-SIGHT HAS
691 REM **** COMPLETELY MISSED THE QFJ SET; DOT IS SET TO SHOW DEEP SPACE
700 DS(J)=DS(J)+BI
710 BI=BI*2
720 NEXT I
740 NEXT J

```

[continued]

[program II continued]

```

790 REM **** 800-920 PRINT THE H-TH LINE OF THE DISPLAY, USING DATA
791 REM **** IN DS AND SH TO PRINT SHADOW (ONCE) AND DEEP SPACE (TWICE).
800 FOR K=1 TO 3
810 LPRINT CHR$(27);CHR$(83);CHR$(48);CHR$(53);CHR$(48);CHR$(48);
820 IF K>2.5 GOTO 850
830 FOR J=1 TO 500
835 LPRINT DS(J));
840 NEXT J
845 GOTO 900
850 FOR J=1 TO 500
855 LPRINT SH(J));
860 NEXT J
900 LPRINT CHR$(13);
910 NEXT K
920 LPRINT CHR$(13)
950 NEXT H
999 END
1000 REM **** THIS SUBROUTINE COMPUTES D, A LOWER BOUND ON THE DISTANCE
1001 REM **** FROM THE CURRENT XYZ (AND T, FIXED) POSITION TO THE QFJ SET
1002 REM **** THE FUNCTION F(Q)=Q*Q-MU IS ITERATED UP TO M TIMES, STARTING
1003 REM **** WITH Q=(X,Y,Z,T); IF THE ESCAPE RADIUS LINF IS EXCEEDED AT
1004 REM **** ANY ITERATION, D IS COMPUTED AT 1200 IN SUCH A WAY THAT ANY
1005 REM **** POINT WITHIN D OF THE STARTING POSITION WOULD ALSO BE EJECTED
1006 REM **** AT THAT STAGE (LIP ESTIMATES THE LIPSCHITZ CONSTANT OF THE
1007 REM **** K-TH ITERATE OF F); IF EJECTION DOES NOT OCCUR AFTER M
1008 REM **** ITERATIONS, D IS SET AT 0
1010 XI=X:Y1=Y:Z1=Z:T1=T
1020 LIP=1:K=0
1030 L=SQR(X1*X1+Y1*Y1+Z1*Z1+T1*T1)
1040 IF L>LINF GOTO 1200
1050 K=K+1:IF K>M GOTO 1190
1060 LIP=LIP*2*L:X2=X1
1070 X1=X1*X1-(Y1*Y1+Z1*Z1+T1*T1+M1)
1080 Y1=2*X2*Y1-M2
1090 Z1=2*X2*Z1-M3
1100 T1=2*X2*T1-M4
1110 GOTO 1030
1190 D=0:GOTO 1300
1200 D=DEL+ABS((L-LINF)/LIP)
1300 RETURN

```

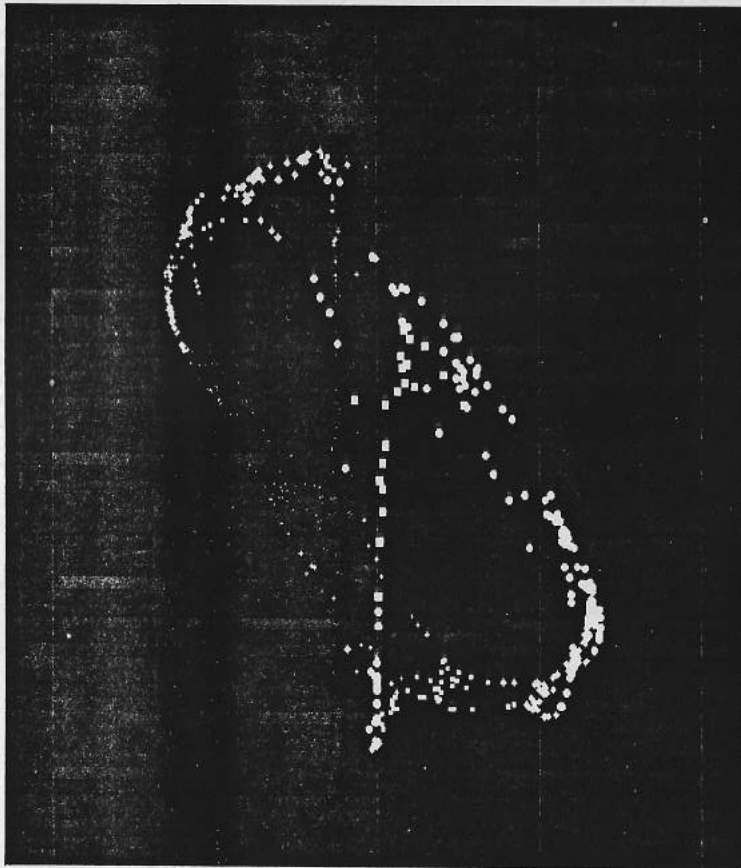


Figure 10: starfield display of QFJ(-1,-1,-1,0)

Program III

```

10 REM **** QFJSTAR.BAS - DISPLAYS QFJ STARFIELDS
20 INPUT "ENTER MU, IE M1,M2,M3,M4: ",M1,M2,M3,M4
30 INPUT "ENTER NUMBER OF ITERATIONS (<10): ",N
35 LPRINT CHR$(27);CHR$(62);
40 INPUT "ENTER SEMIAxis OF PRINTOUT (IN DOTS, <311>): ",D
42 REM **** VECTORS X,Y,Z,T WILL STORE THE COORDINATES OF THE
43 REM **** L (=2 TO THE N-TH) POINTS IN THE N-FOLD INVERSE IMAGE
44 REM **** OF THE STARTING POINT SET IN 80; XD,YD,ZD WILL BE VALUES
45 REM **** DERIVED FROM THE XYZ-PROJECTION, USED FOR A PARTICULAR
46 REM **** DISPLAY OF THE DATA
50 L=2^N
60 DIM X(L),Y(L),Z(L),T(L),XD(L),YD(L),ZD(L)
62 REM **** BY WILL STORE THE BYTES CONTAINING THE BIT-IMAGE GRAPHICS
63 REM **** DATA NEEDED TO PRINT EACH LINE (8 DOTS HIGH) OF THE DISPLAY
64 REM **** BYM WILL BE A MASKED FORM OF BY USED TO PRINT SEGMENTS OF BY
65 DIM BY(621),BYM(621)
66 INPUT "ENTER BACKGROUND COLOR (B/W): ",C#
67 REM **** PER WILL CONTROL SIZE OF STAR IMAGES
68 INPUT "ENTER MAX MAGNITUDE (% OF UPPER LIMIT): ",PER
70 INPUT "ENTER SPIN (ANGLE IN DEGREES): ",TH
72 REM **** 75 SETS PRINTER LINE HEIGHT (ZERO SPACING)
75 LPRINT CHR$(27);CHR$(84);CHR$(49);CHR$(54);
80 X(1)=1:Y(1)=1:Z(1)=0:T(1)=0:LL=1
82 REM **** 90-220 BUILDS UP X,Y,Z,T BY SUCCESSIVE INVERSE IMAGES;
83 REM **** Q IS REPLACED BY (+/-) THE APPROPRIATE QUATERNIONIC
84 REM **** SQUARE ROOT (ROUTINE EXPLAINED ELSEWHERE)
90 FOR J=1 TO N
100 FOR I=1 TO LL
110 X(I)=X(I)+M1:Y(I)=Y(I)+M2:Z(I)=Z(I)+M3:T(I)=T(I)+M4
120 NRM=SQR(Y(I)*Y(I)+Z(I)*Z(I)+T(I)*T(I)):IF NRM>0 GOTO 140
130 U1=1:U2=0:U3=0
135 GOTO 160
140 U1=Y(I)/NRM:U2=Z(I)/NRM:U3=T(I)/NRM
160 MD=SQR(X(I)*X(I)+NRM*NRM)
170 A=SQR(.5*(MD+X(I)))
180 B=SQR(.5*(MD-X(I)))
190 X(I)=A:Y(I)=B*U1:Z(I)=B*U2:T(I)=B*U3
200 X(I+LL)=-X(I):Y(I+LL)=-Y(I):Z(I+LL)=-Z(I):T(I+LL)=-T(I)
205 NEXT I
210 LL=2*LL
220 NEXT J
250 REM **** DISPLAY ROUTINE
251 REM **** M IS THE LENGTH (IN DOTS) OF DISPLAY LINE
252 REM **** SA IS THE INTERNAL VALUE OF THE SEMI-AXIS OF THE
253 REM **** DISPLAY CUBE (SA = 'ESCAPE RADIUS' SO CUBE SHOULD
254 REM **** CONTAIN THE QFJ SET)
260 M=1+2*D:LPRINT:LPRINT
300 THR=TH*3.14159/180:CO=COS(THR):SI=SIN(THR)
304 LMU=SQR(M1*M1+M2*M2+M3*M3+M4*M4)
306 SA=.52+SQR(LMU+.25)

```

[continued]

[program III continued]

```
307 REM **** 310-330 COMPUTE DISPLAY COORDINATES XD,YD,ZD OF THE
308 REM **** L POINTS, INTRODUCING THE EFFECTS OF PERSPECTIVE AND
309 REM **** ROTATION
310 FOR I=1 TO L
315 XD(I)=X(I)/SA:YD(I)=Y(I)/SA:ZD(I)=Z(I)/SA
320 X=XD(I)*XD(I)=C0*X-SI*ZD(I):ZD(I)=SI*X+C0*ZD(I)
325 XD(I)=XD(I)*(3-ZD(I))/4:YD(I)=YD(I)*(3-ZD(I))/4
330 NEXT I
400 REM **** IN 410 AND FOLLOWING I INDEXES THE DISPLAY LINE
401 REM **** (8 DOTS HIGH)
410 FOR I=1 TO 1+INT(M/8)
415 REM **** 420-440 PICKS OUT THOSE POINTS WHOSE STAR IMAGES
416 REM **** WILL AFFECT THE CURRENT PRINT LINE
420 YB=1-(4+8*I)/D:YT=YB+16/D:YO=YT-4/D
430 FOR K=1 TO L
440 IF (YB)<YD(K) OR YT>YD(K) GOTO 500
442 REM **** 445 AND 451-469 DETERMINE THE SIZE OF THE STAR IMAGE,
443 REM **** DEPENDING ON THE DEPTH OF THE STAR POSITION AND ON
444 REM **** PER, THE % OF THE MAGNITUDE SCALE TO BE USED
445 Z=1-PER*(1-ZD(K))/100
446 REM **** P AND J DETERMINE THE DOT CLOSEST TO THE STAR CENTER
450 P=INT(D*(CY0-YD(K))):J=INT(D*(XD(K)+1))
451 IF Z>.7 GOTO 461 ELSE IF Z>.5 GOTO 462 ELSE IF Z>.3 GOTO 463
452 IF Z>.1 GOTO 464 ELSE IF Z>-.1 GOTO 465 ELSE IF Z>-.3 GOTO 466
453 IF Z>-.5 GOTO 467 ELSE IF Z>-.7 GOTO 468 ELSE GOTO 469
458 REM **** THE VALUES OF R BELOW DETERMINE THE RADIUS (IN DOTS)
459 REM **** OF THE STAR IMAGE
461 R=.5:GOTO 470
462 R=1:GOTO 470
463 R=1.43:GOTO 470
464 R=2:GOTO 470
465 R=2.8:GOTO 470
466 R=2.86:GOTO 470
467 R=3:GOTO 470
468 R=3.2:GOTO 470
469 R=3.42
470 IR=INT(R)
471 FOR DP=-IR TO IR
472 FOR DJ=-IR TO IR:IF DP*DP+DJ*DJ>R*R GOTO 480
473 PL=P+DP:JL=J+DJ
474 IF PL<0 OR 7<PL GOTO 480
475 BY(JL)=BY(JL) OR 2^PL
480 NEXT DJ
481 NEXT DP
490 REM **** LINES 470-481, ABOVE, INSERT IN BY THE BIT DATA
491 REM **** CORRESPONDING TO DOTS IN THE STAR IMAGE
500 NEXT K
```

[continued]

[program III continued]

```
505 REM **** 510-637 IS A PRINTER SPECIFIC ROUTINE FOR DISPLAYING
506 REM **** THE STAR IMAGE DATA IN BY; BY IS MASKED (BYM) AND
507 REM **** PRINTED IN SEGMENTS
510 FOR H=1 TO INT(M/105)+1
515 FOR J=1 TO M
520 BYM(J)=255+((H-1)*105<J AND J<(1+H*105))*255-BY(J))
525 NEXT J
600 LPRINT CHR$(27);CHR$(83);CHR$(48);CHR$(54);CHR$(50);CHR$(49);
605 IF C$="B" GOTO 612
610 FOR J=1 TO M:LPRINT CHR$(BY(J));:NEXT J
611 GOTO 620
612 FOR J=1 TO M:LPRINT CHR$(255-BYM(J));:NEXT J:Q=1-Q
620 FOR J=1 TO 621-M:LPRINT CHR$(0);:NEXT J
625 IF Q$="W" GOTO 638
630 IF Q=1 THEN LPRINT CHR$(13);
635 IF Q=0 GOTO 600
636 LPRINT CHR$(13);
637 NEXT H
638 FOR J=1 TO 621:BY(J)=0:NEXT J
640 LPRINT CHR$(13)
650 NEXT I
700 REM **** LABEL DISPLAY
710 LPRINT:PRINT
720 LPRINT "QUATERNIONIC STARFIELD GENERATED BY QSTAR.BAS":LPRINT
730 LPRINT "XYZ PROJECTION OF N-FOLD INVERSE IMAGE OF (1,1,0,0)":LPRINT
740 LPRINT "UNDER THE FUNCTION MAPPING A QUATERNION Q TO Q*Q-MU":LPRINT
750 LPRINT "HERE N (NO. OF INVERSE ITERATIONS) IS ",N:LPRINT
760 LPRINT "HERE MU IS ",M1,M2,M3,M4:LPRINT
770 LPRINT "HERE THE SEMIAxis OF THE DISPLAY FRAME IS ",D," DOTS"
780 LPRINT
790 LPRINT "THE STARFIELD IS SHOWN IN PERSPECTIVE WITH STARS NEAR":LPRINT
800 LPRINT "THE VIEWER INCREASED IN MAGNITUDE; THE PERCENTAGE OF":LPRINT
810 LPRINT "THE FULL MAGNITUDE SCALE USED HERE IS ",PER:LPRINT
820 LPRINT "THE STARFIELD IS FIRST PLOTTED WITH THE X-AXIS TO THE":LPRINT
830 LPRINT "RIGHT, THE Y-AXIS UP, AND THE Z-AXIS TO THE REAR, BUT":LPRINT
840 LPRINT "THE STARFIELD MAY THEN BE ROTATED FOR BETTER VIEWING":LPRINT
850 LPRINT "CURRENT ANGLE OF ROTATION (TO THE EAST AROUND THE ):LPRINT
860 LPRINT "NORTH-SOUTH Y-AXIS) IS ",TH," DEGREES"
900 REM **** REDISPLAY OPTION
910 INPUT "DO YOU WISH TO REPLOT THIS STARFIELD (Y/N)? ",R$
920 IF R$="N" THEN END
930 PRINT "CURRENT SEMIAxis OF DISPLAY FRAME IS ",D," DOTS"
940 INPUT "ENTER SEMIAxis FOR NEXT DISPLAY: ",D
950 PRINT "CURRENT % OF FULL MAGNITUDE SCALE USED IS ",PER
960 INPUT "ENTER % FOR NEXT DISPLAY: ",PER
970 PRINT "CURRENT SPIN IS ",TH, "DEGREES EAST"
980 INPUT "ENTER SPIN FOR NEXT DISPLAY: ",TH
990 INPUT "ENTER BACKGROUND COLOR FOR NEXT DISPLAY (B/W): ",C$
```

1000 GOTO 250

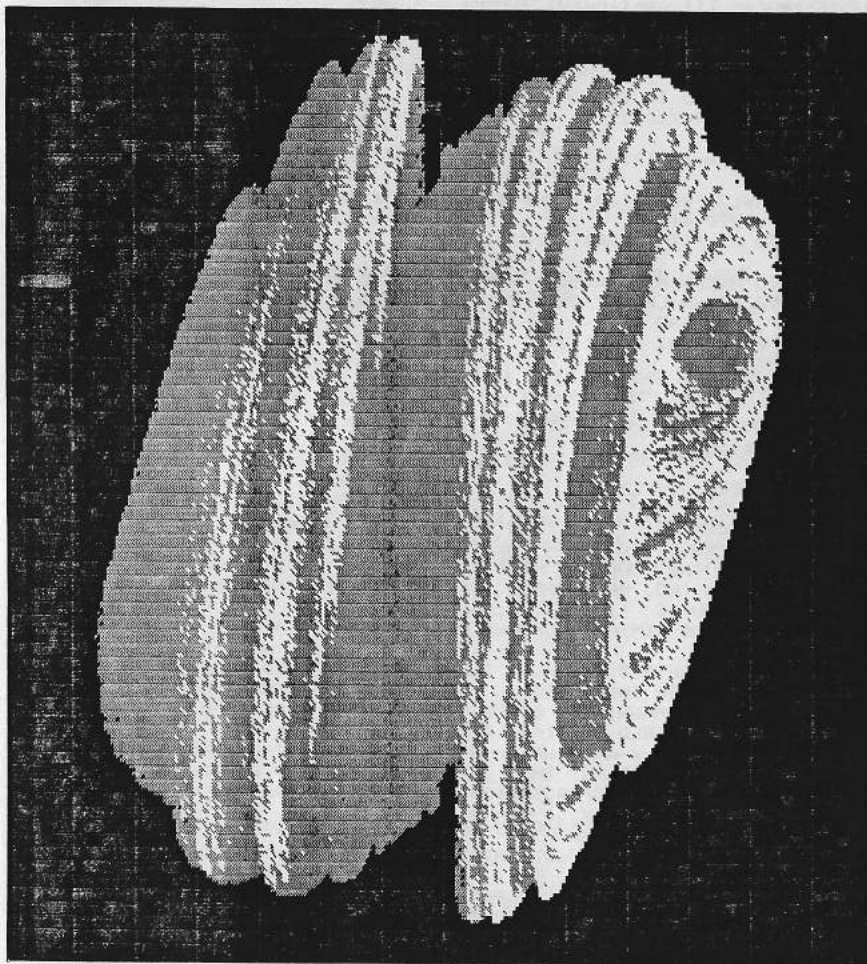


Figure 11: asteroid display of QFJ(-.35,.3,.3,0)

#### References

- [1] E. T. Bell, *The Development of Mathematics* (2nd edition), McGraw-Hill 1945
- [2] C. A. Deavours, *The quaternionic calculus*, Amer. Math. Monthly 80(1973), 995-1008
- [3] S. Eilenberg and I. Niven, The "fundamental theorem of algebra" for quaternions, *Bull. Amer. Math. Soc.* 50(1944), 246-248
- [4] F. Klein, *Elementary Mathematics from an Advanced Standpoint*, Parts I and II, Dover Publications
- [5] B. B. Mandelbrot, *The Fractal Geometry of Nature*, Freeman 1982
- [6] K. Stein, *The fractal cosmos*, Omni 1983
- [7] P. G. Tait, *Quaternions*, 3rd edition, Cambridge Press 1890

Appendix

We are pleased to be able, thanks to some recent correspondence with Benoit Mandelbrot, to update our references to other work on quaternionic fractals. In the second and later printings of [5] there is an "update" section giving a summary of a great variety of new work; included is a short account (all too short!) of results by Mandelbrot and Norton on "the squaring maps in quaternions", and some fascinating new illustrations (see Plate 467, for example). It is clear that there will be many publications in this area, by Mandelbrot and Norton and, no doubt, by others. An article [A1] by Norton is apparently already available.

[A1] V. A. Norton, Generation and display of geometric fractals in 3-D, Computer Graphics 16(1982), 61-67

ROUGH EDGE OF MATH LEADS TO SCENERY BY COMPUTER<sup>+</sup>

by Derek York

To talk to Benoit Mandelbrot is to fall into a kaleidoscope of ideas. Images from mathematics, music, art and physics replace each other in bewildering succession. Yet different as these ideas are, they are linked by a thread which is at once continuous and broken. They are linked by a fractal thread. And Dr. Mandelbrot is the "father of fractals".

In the past decade, Dr. Mandelbrot, an IBM Fellow at the Thomas J. Watson Research Centre in Yorktown Heights, N.Y., has been teaching people how to see the world around them through new eyes. He is the expositor of a new geometry of nature. A nature filled with beauty, but rough at the edges. A nature with fractional dimensions.

For about 2,000 years, it has been the custom to represent the forms of nature via the geometry of the ancient Greeks. The world was regarded as being essentially built up of lines, planes, circles, spheres, cubes, spirals etc., all of which are smooth shapes. The orbit of Jupiter about the sun, for instance, is an ellipse. The Earth's shape is approximately spherical. Bobby Hull's slap-shot seemed to travel almost in a straight line. The DNA molecule is a double helix. And so on.

In contrast with these observations, however, Dr. Mandelbrot asks: How would you approximate the irregular surface of a layer of cloud beneath an aircraft? How would you represent mathematically the interfingering network of streams draining a mountainous area? How would you describe the mountains themselves, come to that? How do you model the architecture of a tree? Could you represent the water cascading down the falls at Niagara with a natural combination of straight lines and circles?

In answer, the famous mathematician would claim that these various natural phenomena, and many others in such realms as physics, chemistry and biology, are most naturally described by "fractals." These are shapes or surfaces or curves which are continuous, but broken on the finest of scales (Dr. Mandelbrot coined the word fractal from the Latin fractus, meaning broken).

Such curves had been known to mathematicians for many years, but had generally been regarded as "pathological" or "monstrous" because of their peculiar properties. While they were mathematically fascinating, it was not generally felt that they were of any use in representing the real world. What Dr. Mandelbrot has proposed is that in fact such curves are not exceptional "monsters."

They are all around. His favorite way of illustrating this is with the "snowflake" curve invented by Helge von Koch in 1904.

<sup>+</sup> This article appeared earlier in the Toronto Globe and Mail.  
Friday, April 8th, 1983.

This fractal is constructed by the series of small black figures shown on this page. You begin with a triangle whose sides are all of the same length. A similar triangle is then added at the middle of each side, to give a Star of David. A similar but smaller triangle is then added to each side of the Star of David and so on ad infinitum.

In the end, then, a continuous curve will have been generated. Yet on every scale at which we might inspect it, with ever more powerful microscopes, it would be continually changing direction.

What makes the curve even more bizarre is the fact that while the area inside the curve tends towards a definite value as the "snowflake" gains greater details, the length of the curve increases to infinity. No wonder such curves were called "monsters" and considered to have no counterpart in nature.

If you are inclined to agree with this, then you are wrong, says the IBM mathematician. The coastline of British Columbia (or any coast line) is very well represented by a modified piece of the "snowflake" curve, a Koch curve. Take the stretch from New Westminster to Prince Rupert. As the crow flies, this distance is about 800 kilometres (500 miles). But if you measured this distance along the coastline with a ruler which was 80 km (50 miles) long, you would find a length significantly greater than 800 km.

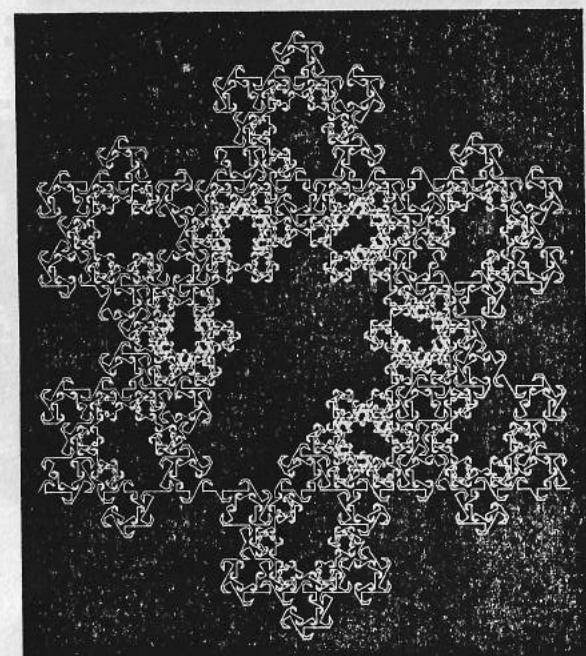
And if you followed the coastline with a one-foot ruler, you would cover a distance far beyond 800 km. If you repeated this process endlessly with ever smaller rulers, you would find the stretch of coastline was becoming longer and longer.

This behavior, says Dr. Mandelbrot, is just like that of a Koch curve. This is completely different from the behavior of a smooth curve such as a circle. If we measured an arc on a circle in the same way that we used for the British Columbia coastline, we would very quickly find that our repeated measurement of length rapidly converged and after a while showed essentially no change.

Surely then, says Dr. Mandelbrot, it's more reasonable to represent coastlines by fractals than by smooth curves.

The obvious similarity between coastlines and Koch curves is that they both show more and more fine structure as you examine them on finer and finer scales.

The obvious difference is that the Koch curve is boring, showing more and more of the same thing as you look at it more closely. Whereas the coastline, while showing bays, sub-bays and sub-sub-bays, and promontories, sub-promontories and sub-sub-promontories is not, of course, identical at all magnifications. To model coastlines fractally more accurately, therefore, Dr. Mandelbrot paradoxically allows chance to enter his calculations and produces extraordinarily convincing models of coastlines, rivers, mountains, lakes and islands. His fractally generated planet-scapes inspired scenes in the movie Star-Trek2.



But this extraordinary mathematician thoughts are not bounded by coastlines (infinitely long or otherwise). He brings within the fractal realm, galaxies, turbulence in the atmosphere, problems in condensed matter physics, the folding in space of giant molecules, price changes in economies, music and art. The intricate network of blood vessels in the lung is imitated with the so-called "monster Peano curve" invented by Giuseppe Peano in 1890.

In a recently published tour de force, *The Fractal Geometry of Nature*<sup>+</sup> (W.H. Freeman and Co., San Francisco), Dr. Mandelbrot displays many spectacular illustrations of computer-drawn fractals. For scientists and artists alike, it is a feast for the eye as well as the mind. What a far cry from the art inspired by the Golden Mean of the Greek geometers.

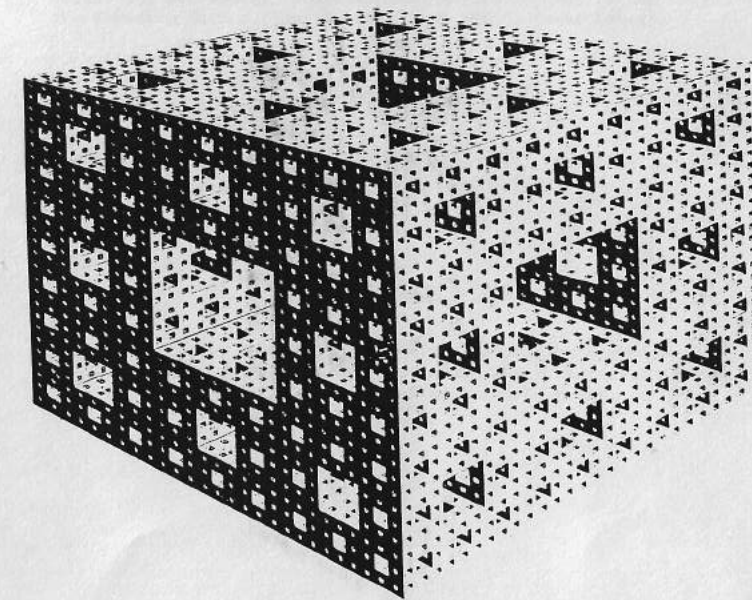
One of the most striking achievements of Dr. Mandelbrot is to have brought some of the most esoteric of mathematical concepts into the popular domain. At age 58, he is a hot item on the lecture circuit. He was in Ontario last month to headline a week-long seminar on mathematical physics at the University of Guelph where his public lecture on fractals drew a large audience including many schoolchildren.

Currently he is a consultant for the science centre being planned in Paris, where French planners hope to have a fractals display.

Why does he work at IBM rather than in a university environment? "Firstly, university departments are usually divided into well-defined groups of specialists, whereas my interests span many fields. Secondly, before fractals took off, it would have been very difficult to get funding for my research from the U.S. National Science Foundation."

After leaving Guelph, he was flying to Boston to visit the well-known seismologist K. Aki to talk about fractals and earthquakes and to accept an invitation to be an associate editor of a geophysical journal. "I'm becoming a geophysicist now, he said, with a smile.

<sup>+</sup> Our thanks to Dr. Mandelbrot for his permission to reproduce the figures that accompany this article.



SUBSCRIPTIONS

The subscription rate for the Applied Mathematics Notes is \$6.00 (Canadian) per annum. Subscriptions should be sent to the office of the Canadian Mathematical Society (see inside front cover).

ABONNEMENT

Abonnement annuel: 6 dollars canadiens. Faire parvenir le paiement au bureau de la Société Mathématique du Canada.

INSTRUCTIONS TO AUTHORS

Since the Applied Matheamtics Notes are printed by a photo-offset process, authors are requested to submit the original typescript (plus one copy) on 8 1/2 by 11 or A4 paper.

Printed at

Imprimé à:

University of Guelph, Guelph, Ontario N1G 2W1